Mantle heterogeneity from trace elements: MAR triple junction near 14°N

Article *in* Earth and Planetary Science Letters · April 1988

DOI: 10.1016/0012-821X(88)90043-X

6 authors, including:

Henri Bougault
Institut Français de Recherche pour l'Exploitation de la Mer
397 PUBLICATIONS **5,023** CITATIONS

SEE PROFILE

Jean-Guy Schilling
University of Rhode Island
195 PUBLICATIONS **12,783** CITATIONS

SEE PROFILE

Alexander V Sobolev
Université Grenoble Alpes
257 PUBLICATIONS **9,347** CITATIONS

SEE PROFILE

J.-L. Joron
Paris Diderot University
305 PUBLICATIONS **10,883** CITATIONS

SEE PROFILE

Earth and Planetary Science Letters, 88 (1988) 27–36
Elsevier Science Publishers B.V., Amsterdam – Printed in The Netherlands

[4]

Mantle heterogeneity from trace elements: MAR triple junction near 14° N

H. Bougault [1], L. Dmitriev [2], J.G. Schilling [3], A. Sobolev [2], J.L. Joron [4] and H.D. Needham [1]

[1] *IFREMER, Centre de Brest, B.P. 337, 29273 Brest Cedex (France)*
[2] *Vernadsky Institute of Geochemistry, U.S.S.R. Academy of Sciences, Kosigina 19, Moscow W 334 (U.S.S.R.)*
[3] *Graduate School of Oceanography, University of Rhode Island, Narragansett, RI 02882 (U.S.A.)*
[4] *Laboratoire P. Sue, C.N.R.S. C.E.N. Saclay, B.P. 2, 91192 Gif-sur-Yvette (France)*

Received September 1, 1987; revised version accepted January 4, 1988

The trace element composition of basalts dredged at the axis of the Mid-Atlantic Ridge between 12° N and 17° N by the R/V "Akademik Boris Petrov" demonstrates the presence of a high-amplitude geochemical anomaly, centered around 14° N and extending at least 300 km along the strike of the Rift Valley. The anomaly does not fit easily into any of the models that have been proposed: it may reflect the upwelling of an embryonic mantle plume or of a passive mantle domain responsible for or associated with a triple junction, possibly marking a recent shift into the area of the South American/North American plate boundary.

1. Introduction

It is now well established that along the Mid-Atlantic Ridge (MAR) in the North Atlantic regional variations of isotopic ratios such as $^{87}Sr/^{86}Sr$ or $^{143}Nd/^{144}Nd$ and normalized ratios of highly to less magmaphile elements, $(La/Sm)_N$, $(Nb/Zr)_N$, $(Ta/Hf)_N$, coincide with major anomalous elevations of zero age crust and with positive residual gravity anomalies [1–9] (Fig. 1). These anomalies have been interpreted in terms of plumes upwelling close to, or directly beneath, the MAR axis and usually referred to as ridge-centered hotspots.

Relationships among the geochemical and geophysical parameters are complex [10,11]. The number of mantle components which need to be invoked in order to explain data on radiogenic isotopes, trace elements and rare gases, is increasing as new data become available. The sizes of identified domains vary from the dimensions of an ocean [12] to those of local heterogeneities within a single dredge or a single drill core [13]. In the North Atlantic, gradients of trace element and of radiogenic isotope ratios are observed correlatively with gravity and with ridge elevation at an along-strike scale of about 1000 km, centered on Iceland and on the Azores triple junction (Fig. 1) [1–5]. Smaller geochemical gradients or anomalies (300 km or even spike like) have also been observed along the MAR (8°30′S, 16°S [14,15], 35° N [3,16]), apparently without corresponding ridge centered gravimetric anomalies and with more subdued bathymetric anomalies. In the South Atlantic, the zero-age geochemical anomalies tend to be located facing off-ridge hotspots (Tristan, St. Helena, Circe) [11,15].

The Mid-Atlantic Ridge between 20° N and 5° S has remained too poorly sampled to document significant variations of geochemical characteristics of the oceanic crust and mantle. It is of interest to note that, on kinematic evidence, this section of the MAR should include the triple junction of the boundaries between the North American, South American and African plates, but the exact location remains enigmatic [17]. The southern part of the 5° S to 20° N MAR region includes long, closely spaced fracture zone offsets which may, for thermal reasons, affect magma the formation and emplacement of the new oceanic crust [18–21].

In order to complete the existing MAR sampling gap between 20° N and 5° S and further study the relationships between geochemical

Contribution No. 103 de l'IFREMER Centre de Brest.

0012-821X/88/$03.50

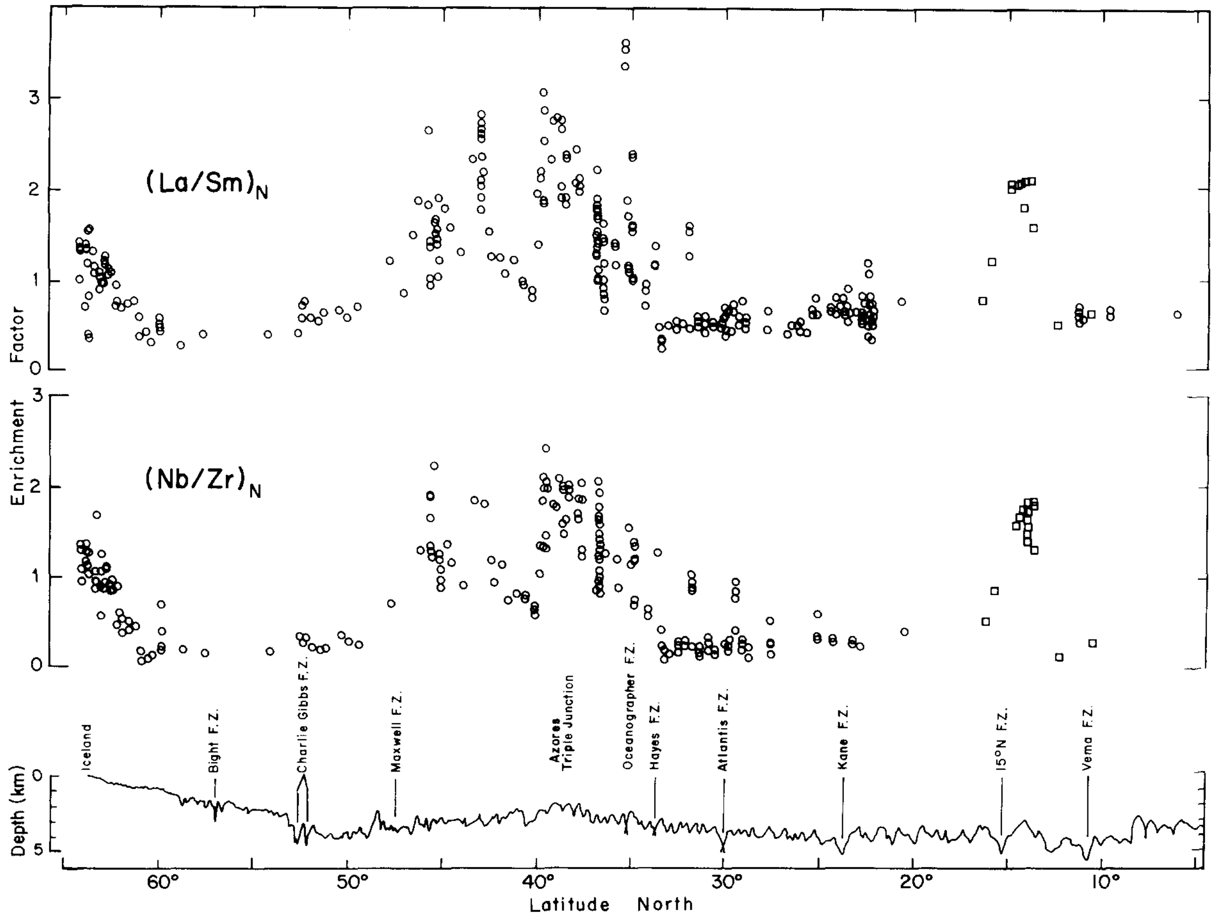

Fig. 1. The "chemical structure of the Mid-Atlantic Ridge". $(La/Sm)_N$, $(Nb/Zr)_N$ chondrite-normalized ratios and the zero-age depth are plotted versus latitude. Note the striking correlations between the chemical parameters themselves and the ridge bathymetry: hence the expression "chemical structure". The 14° N ridge chemical anomaly corresponds to a bathymetric bulge at this latitude. Note also the scarcity of chemical data between 20° N and the equator; circles correspond to various data available prior to this study; squares represent new data reported in the present study (14° N area). The bathymetric curve between 40° and 10° N is from Needham ([24] and unpublished). The extension of it is from Gente [25].

parameters, geology and geophysics of the ocean crust, a cooperative programme was set up by scientists of the Vernadsky Institute of Geochemistry (U.S.S.R.), the University of Rhode Island (U.S.A.) and IFREMER (France). In this article, we report new data concerning the MAR in the vicinity of 14° N which are based on results of a cruise in April-May 1985 of the R/V "Akademik Boris Petrov".

2. Geologic setting

Kinematic plate models point to differential motions of South America with respect to North America as well as Africa, thus implying the presence of a triple junction on the MAR. Minster and Jordan's [17] solution indicates that it lies between 10° and 20° N. Recent syntheses by Collette and coworkers (e.g. [20]) has led them to suggest that the triple junction moved into the area only about 7 My ago, having been previously located near 8° N. They argue that the accompanying change in spreading direction produced compression in the Barracuda Ridge zone (Fig. 2), and led to north-south extension closer to the MAR crest amounting to 18 km and giving rise to the off-axis complex represented by Researcher Ridge and Researcher Trough (near 14° N) and the Royal

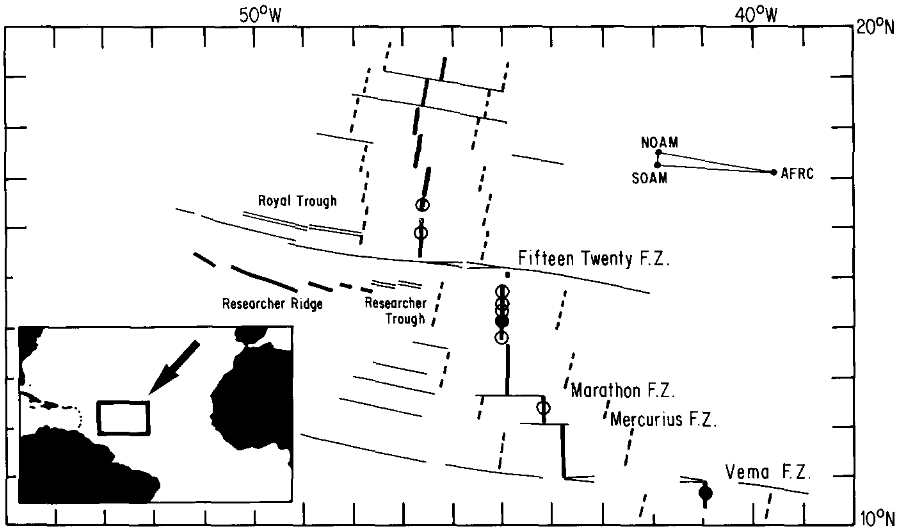

Fig. 2. Tectonic configuration of the 14° N MAR Triple Junction from Roest and Collette [20]. The vector diagram shows direction and velocity of relative motions of the North American, South American and African plates. Dashed lines represent the Ridge axis 7 My ago, indicating the change in spreading direction. Dredge locations during Leg 2 of the R/V "Akademik Boris Petrov" are indicated by open circles. Dots are the locations of dredge hauls by the R/V "J. Charcot" (CH 77 and CH 78).

Trough (just north of the 15° 22′N Fracture Zone) (Fig. 2). These features appear to be made up of graben and en-echelon units which trend approximately along the spreading direction (flow lines) west of the MAR (Fig. 2). A volcano-tectonic origin is compatible with large magnetic anomalies recorded on the Researcher Ridge [21] and by Gloria data on the Royal Trough (Searle's communication referred to in Roest and Collette [20]).

Roest and Collette [20] consider that the triple junction must lie to the north of the 15° 20′N Fracture Zone, near 16° N. Le Douaran and Francheteau [22], although noting that the whole region between 10° N and 20° N may have been affected by motion between North America, South America and Africa, tentatively place the inferred triple junction near 14° N, where a shallow rift valley coincides with a geochemical anomaly reported by one of us on the basis of a single dredge haul [23]. The along strike depth curve established by Needham ([24] and Fig. 1) does not itself provide clear evidence of the location of a triple junction at the ridge axis at 14° N; however, the curve shows that whether a local feature or the highest area of a broader zero-age zone, the bathymetric high at 14° N includes the shallowest part of the rift valley floor so far found between 10° and 20° N. The deepening, from the top of the bulge towards adjacent fracture zones, corresponds to a 2000 m per degree of latitude along strike on either side of the 14° N peak. With this background in mind, the objective of our sampling during the "Akademik Boris Petrov" cruise was to define the geochemical anomaly at 14° N and to map its extent to the north and south.

3. Methodology

The locations of our dredged samples (Fig. 2), controlled by Seabeam soundings, are on the inner floor of the MAR rift valley, where small volcanic structures oriented along strike represent recent eruptions. The freshness and glassy nature of most of the basalts recovered confirmed their young age.

Most of the samples selected for shipboard chemical analyses and further on shore investigations are either glasses or aphyric basalts, as specified in Table 1. Many of them showed a gain in weight after ignition at 1050° C (Table 1) indicating an oxygen uptake (mainly Fe^{2+} oxidation) larger than the loss in volatiles, which is another indication of the freshness of the samples. Among these samples, was a highly vesicular glass (2ΠD

TABLE 1

Major and trace element compositions of Mid-Atlantic Ridge basalts from 10° N to 17° N [a]

Major elements

Sample	Type [b]	Lat. ° N	Long. ° W	Depth (m)	SiO_2	Al_2O_3	PtO^T	MnO	MgO	CaO	Na_2O	K_2O	TiO_2	P_2O_5	LOI	*D*
CH78-08-13	I	10.62	40.83	4339	49.70	14.65	11.59	0.20	7.12	10.27	3.29	0.21	2.19	0.23	−0.29	269.91
CH78-08-20	I	10.62	40.83	4339	50.18	14.73	11.53	0.20	7.15	10.34	3.40	0.21	2.20	0.22	−0.28	274.06
CH78-08-23	I	10.62	40.83	4339	49.23	19.58	7.37	0.12	7.30	12.63	2.53	0.21	1.19	0.13	0.00	254.38
CH78-08-26	I	10.62	40.83	4339	49.95	19.35	7.31	0.13	7.01	12.62	2.91	0.14	1.15	0.10	−0.12	263.62
CH78-08-27	I	10.62	40.83	4339	49.91	14.70	10.62	0.19	7.67	10.68	3.31	0.15	2.00	0.22	−0.70	273.54
CH78-08-46	I	10.62	40.83	4339	50.31	14.77	11.71	0.20	6.79	10.40	3.58	0.38	2.22	0.22	−0.04	270.47
2ΠD 40-1	G	12.40	44.10	4375	50.85	15.33	9.50	0.16	8.65	12.03	2.55	0.06	1.37	0.13	−0.73	263.72
2ΠD 40-2	G	12.40	44.10	4375	49.46	15.00	10.18	0.16	8.53	11.57	2.35	0.05	1.61	0.16	−0.86	257.86
2ΠD 43-1	I	13.77	45.01	3770	50.57	14.50	10.10	0.16	8.41	10.77	2.87	0.67	1.83	0.31	−0.25	251.46
2ΠD 43-1LV	G	13.77	45.01	3770	50.41	14.33	9.89	0.15	8.33	10.52	3.03	0.70	1.79	0.27	–	251.51
2ΠD 43-1HV	G	13.77	45.01	3770	49.96	14.28	9.92	0.15	8.28	10.65	3.03	0.70	1.79	0.28	–	250.07
2ΠD 43-3	I	13.77	45.01	3770	51.13	14.65	9.85	0.16	9.61	11.07	2.41	0.26	1.37	0.18	−0.56	255.92
CH77-06-119	I	14.12	45.00	2954	50.13	15.44	9.81	0.17	7.57	11.65	2.45	0.59	1.44	0.23	−0.07	239.42
CH77-06-124	I	14.12	45.00	2954	51.50	15.39	9.41	0.17	7.39	11.71	2.45	0.61	1.48	0.23	0.00	243.75
CH77-06-125	I	14.12	45.00	2954	50.51	15.73	9.32	0.16	7.66	12.09	2.49	0.56	1.34	0.20	0.12	242.66
CH77-06-126	I	14.12	45.00	2954	50.42	15.53	9.59	0.17	7.34	11.64	2.45	0.61	1.46	0.21	0.16	239.70
CH77-06-157	G	14.12	45.00	2954	50.92	15.41	9.55	0.17	7.63	11.55	2.45	0.51	1.44	0.21	−0.35	244.94
CH77-06-201	I	14.12	45.00	2954	48.51	15.52	8.82	0.16	10.56	12.19	1.92	0.37	1.00	0.16	0.13	236.67
CH77-06-203	I	14.12	45.00	2954	49.13	16.02	9.23	0.16	9.47	12.14	1.98	0.43	1.05	0.16	0.09	235.03
CH77-06-205	I	14.12	45.00	2954	50.55	16.64	9.10	0.15	6.16	11.57	2.51	0.64	1.60	0.26	0.13	240.53
2ΠD 44-1	G	14.33	45.04	3090	51.94	15.35	9.74	0.17	7.56	10.85	2.83	0.57	1.63	0.23	–	254.00
2ΠD 44-3	G	14.33	45.04	3090	51.46	15.31	10.24	0.17	6.74	10.76	2.78	0.61	1.88	0.27	−0.27	251.16
2ΠD 45-1	I	14.50	44.84	3720	51.76	14.89	9.49	0.16	7.32	10.83	2.77	0.69	1.71	0.26	0.48	248.95
2ΠD 45-2	G	14.50	44.84	3720	51.68	14.71	9.82	0.16	7.52	10.74	2.68	0.57	1.69	0.24	−0.28	250.69
2ΠD 46-2	I	14.71	45.02	3950	50.32	16.97	8.03	0.14	7.67	11.91	2.62	0.61	1.29	0.16	–	244.66
2ΠD 46-3	I	14.71	45.02	3950	51.33	14.80	9.84	0.17	7.40	10.75	2.58	0.74	1.68	0.24	–	241.85
2ΠD 47-1	G	15.88	46.58	3760	50.38	14.77	9.43	0.17	8.25	10.80	2.81	0.29	1.53	0.19	−0.57	258.02
2ΠD 48-1	G	16.34	46.66	3500	50.14	14.24	10.62	0.18	8.13	10.58	3.01	0.19	1.72	0.17	−0.70	264.12
2ΠD 48-3	G	16.34	46.66	3500	50.49	14.32	10.45	0.18	7.92	10.48	3.09	0.21	1.71	0.17	−0.03	265.23
2ΠD 48-4	G	16.34	46.66	3500	50.58	14.10	10.49	0.18	8.03	10.56	3.03	0.21	1.72	0.17	0.17	265.04

Magmaphile trace elements

Sample	Type [b]	Th [c]	La [c]	Ta [c]	Nb [d]	Nb [e]	Zr [d]	Zr [e]	Hf [c]	Ti [e]	Y [e]	$(Nb/Zr)_N$	$(Ta/Hf)_N$
CH78-08-13	I	0.19	5.1	0.24	–	5.0	–	171	4.54	12960	50.0	0.30	0.22
CH78-08-20	I	0.19	4.9	0.24	–	5.6	–	176	4.36	13020	50.0	0.33	0.23
CH78-08-23	I	0.38	2.6	0.12	–	2.2	–	83	2.13	7080	27.0	0.27	0.24
CH78-08-26	I	0.23	2.3	0.11	–	2.1	–	77	2.05	6840	27.0	0.28	0.22
CH78-08-27	I	0.39	4.5	0.23	–	4.7	–	151	3.94	11880	45.0	0.32	0.24
CH78-08-46	I	0.21	5.1	0.24	–	5.5	–	177	4.42	13140	50.0	0.32	0.23
2ΠD 40-1	G	0.08	2.3	0.09	0.5	1.0	84.0	90	2.40	8160	33.0	0.11	0.16

2ΠD 40-2	G	0.11	2.6	0.11	1.1	2.1	114.0	116	3.20	9540	41.0	0.19	0.14
2ΠD 43-1	G	1.29	12.9	1.59	25.6	25.5	137.8	136	3.40	10860	32.0	1.92	1.96
2ΠD 43-1LV	G	1.49	13.2	1.64	26.7	24.9	142.5	134	3.50	10620	32.0	1.91	1.96
2ΠD 43-1HV	G	1.40	13.3	1.63	26.3	24.9	139.7	140	3.40	10620	32.0	1.82	2.00
2ΠD 43-3	I	0.47	6.2	0.67	11.6	10.9	88.7	85	2.30	8160	28.0	1.18	1.22
CH77-06-119	I	1.14	10.0	1.25	–	18.6	–	117	2.49	8520	25.5	1.63	2.10
CH77-06-124	I	1.19	10.2	1.23	–	20.1	–	110	2.60	8760	26.1	1.87	1.98
CH77-06-125	I	1.02	9.2	1.12	–	18.1	–	103	2.34	7980	26.4	1.80	2.01
CH77-06-126	I	1.12	10.1	1.20	–	18.2	–	102	2.53	8460	26.0	1.83	1.99
CH77-06-157	G	1.13	10.6	1.21	–	19.6	–	108	2.47	8520	25.8	1.86	2.05
CH77-06-201	I	0.65	6.0	0.68	–	10.8	–	74	1.57	5940	22.0	1.50	1.81
CH77-06-203	I	0.69	6.1	0.73	–	11.7	–	84	1.80	6240	24.2	1.43	1.70
CH77-06-205	I	1.27	12.0	1.35	–	20.6	–	122	2.94	9480	26.1	1.73	1.92
2ΠD 44-1	G	1.27	11.6	1.30	–	–	–	–	3.00	9660	–	–	1.82
2ΠD 44-3	G	1.20	12.6	1.45	23.0	23.3	128.4	136	3.20	11660	29.0	1.76	1.90
2ΠD 45-1	I	1.28	12.0	1.38	21.4	20.6	133.7	128	3.10	10140	29.0	1.65	1.87
2ΠD 45-2	G	1.31	12.6	1.38	21.7	20.9	131.3	127	3.30	10020	28.0	1.69	1.75
2ΠD 46-2	I	0.80	8.6	0.94	15.6	14.4	87.0	91	2.10	7740	21.0	1.62	1.88
2ΠD 46-3	I	1.10	11.7	1.32	21.1	20.5	133.3	131	3.10	10020	30.0	1.61	1.78
2ΠD 47-1	G	0.65	6.7	0.62	10.0	11.2	116.7	116	2.90	9420	33.0	0.99	0.90
2ΠD 48-1	G	0.35	4.9	0.40	4.9	7.7	120.6	119	3.30	10560	41.0	0.66	0.51
2ΠD 48-2	I	0.52	5.0	0.39	6.8	5.8	120.0	127	3.10	–	41.0	0.47	0.53
2ΠD 48-3	G	0.34	4.7	0.42	6.2	6.9	124.5	127	3.30	10200	41.0	0.55	0.53
2ΠD 48-4	G	–	–	–	5.9	6.1	102.0	114	–	10380	38.0	0.55	–
Normalization values		0.028	0.32	0.031	0.5	0.5	5.13	5.13	0.13	460	2.16		

Rare earths and 1st transition elements [f]

Sample	Type [b]	La	Ce	Nd	Sm	Eu	Gd	Tb	Dy	Yb	Lu	Sc	V	Co	Cr	$(La/Sm)_N$
2ΠD 40-2	I	3.03	11.09	11.30	4.36	1.365	6.17	1.080	7.34	4.21	0.585	36	314	42	278	0.49
2ΠD 43-2	I	14.22	33.48	19.60	4.76	1.613	6.59	0.992	5.36	2.97	0.432	35	275	44	253	2.09
CH77-06-157	I	10.42	23.01	13.23	3.52	1.234	–	0.745	–	2.22	0.287	37	251	39	286	2.07
CH77-06-201	I	6.44	15.77	9.16	2.52	0.924	3.75	0.589	3.56	2.11	0.319	38	238	47	837	1.79
2ΠD 44-1	I	12.92	30.00	16.99	4.41	1.497	–	0.846	5.37	2.63	0.338	37	290	41	240	2.05
2ΠD 45-2	I	13.62	30.05	16.77	4.70	1.448	5.92	0.894	4.82	2.74	0.379	35	291	39	240	2.03
2ΠD 47-1	I	7.61	19.19	–	4.43	1.457	6.29	0.968	5.81	3.45	0.466	37	283	42	239	1.20
2ΠD 48-1	I	5.36	16.19	–	4.84	1.619	7.45	1.162	6.65	4.17	0.619	38	307	45	250	0.78
Normalization values [g]		0.30	0.84	0.58	0.21	0.074	0.32	0.049	0.31	0.18	0.025					

[a] All major element concentrations in (wt.%): FeO^T is total iron as FeO; LOI is loss of volatiles on ignition between 100 and 1050 °C; D is discriminant function as defined in [46,47]; and other trace element concentrations are in ppm.

[b] Type: G = basalt glass, I = interior of pillow or sheet flow basalt.

[c] Epithermal neutron activation analyses; Laboratoire Pierre Sue, France.

[d] X-ray fluorescence analyses, on-board R/V "Akademik Boris Petrov", Leg 2.

[e] X-ray fluorescence analyses, on-shore, IFREMER, France.

[f] Instrumental neutron activation analyses, URI, U.S.A. (analyst B. McCully).

[g] Used for calculating listed normalized ratios (e.g. $(La/Sm)_N$).

43-1HV), which was still freely popping on the deck as it was degassing from its recent decompression [26].

Major elements and Nb and Zr concentrations were determined on board the "Akademik Boris Petrov" by X-ray fluorescence spectrometry according the procedure described by Bougault and coworkers [27–30]. The $(Nb/Zr)_N$ normalized ratio provides the same information as the $(La/Sm)_N$ normalized ratio about the level of enrichment or depletion of MORBs [5,23]. Such measurements provide key information on potential heterogeneities as a sampling cruise is progressing [5,10]. For post-cruise confirmation, the rate earth element concentrations were determined on the same samples by neutron activation analysis at the University of Rhode Island [31], and La, Th, Ta and Hf concentrations were measured at the Laboratoire Pierre Sue using epithermal neutron activation [32]. All these results, together with our previous data, are presented in Table 1, along with the exact location and depth of recovery of dredged samples.

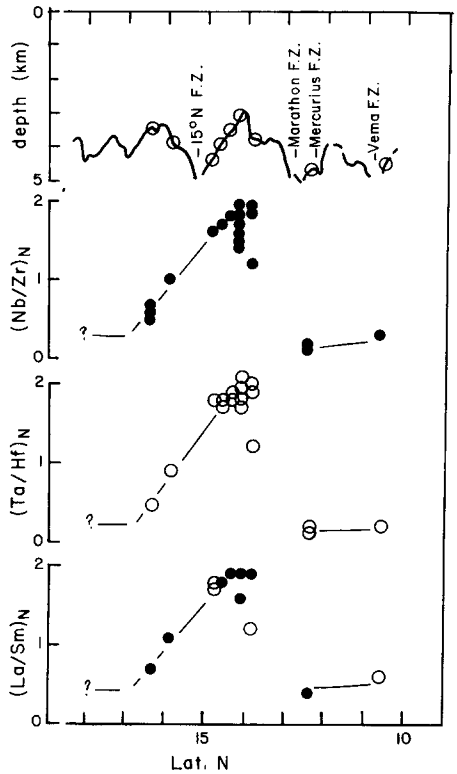

Fig. 3. MAR zero age depth and variation of trace element ratios between 10°N and 17°N. Open circles on the upper part of the figure indicate dredge locations. $(Nb/Zr)_N$, $(Ta/Hf)_N$ and $(La/Sm)_N$ ratios are chondrite-normalized ratios. On the lower part of the figure, the $(La/Sm)_N$ diagram, open circles correspond to $(La/Ti)_N$ as substitutes of $(La/Sm)_N$: see Fig. 4 for justification. Bathymetry from Needham ([24] and unpublished).

4. Along-ridge geochemical variations

The major element data (Table 1) indicate that all basalts dredged between 10°N and 17°N are typically tholeiitic in composition and the FeO/MgO ratio shows no evident variation with respect to distance to fracture zones, or rift floor elevation: but it should be noted that sampling density remains sparse and the intervals between stations are irregular. In contrast, the $(Nb/Zr)_N$ normalized ratio shows a clear latitudinal change (Fig. 3). Magmaphile element enriched basalts, with $(Nb/Zr)_N$ ratios similar in magnitude to those found around the FAMOUS-Azores triple junction [5,23], are located between the Marathon (12°45′N) and the 15°20′N Fracture Zones. Basalts recovered just south of the Marathon Fracture Zone (2ΠD 40), on the short segment between the Marathon and Mercurius (12°10′N) Fracture Zones, have a very low $(Nb/Zr)_N$ (0.2) and unusually depleted character for MAR basalts, similar in this respect to samples recovered at site 504B on the Costa Rica Rift [33,34]; samples collected immediately south of the Vema Fracture Zone also are depleted. North of the 15°20′N Fracture Zone basalts have chondritic to depleted ratios suggesting a possible gradient extending across the 15°20′N Fracture Zone if interpolation is made between stations. At any rate, the latitudinal $(Nb/Zr)_N$ variations demonstrate that all basalts of the 14°N ridge segment have an enriched character compared to those of adjacent segments.

Shipboard conclusions based on $(Nb/Zr)_N$ ratios are fully confirmed by the latitudinal variations of $(La/Sm)_N$ and $(Ta/Hf)_N$ chondrite-normalized ratios, which were determined on shore on the same samples. The striking similarity in the $(Nb/Zr)_N$, $(Ta/Hf)_N$ and $(La/Sm)_N$ latitudinal profiles underlines the similar behavior of these three pairs of elements during mantle evolution and MORB genesis (Fig. 3). Fig. 4 illustrates the large differences that exist between the enriched

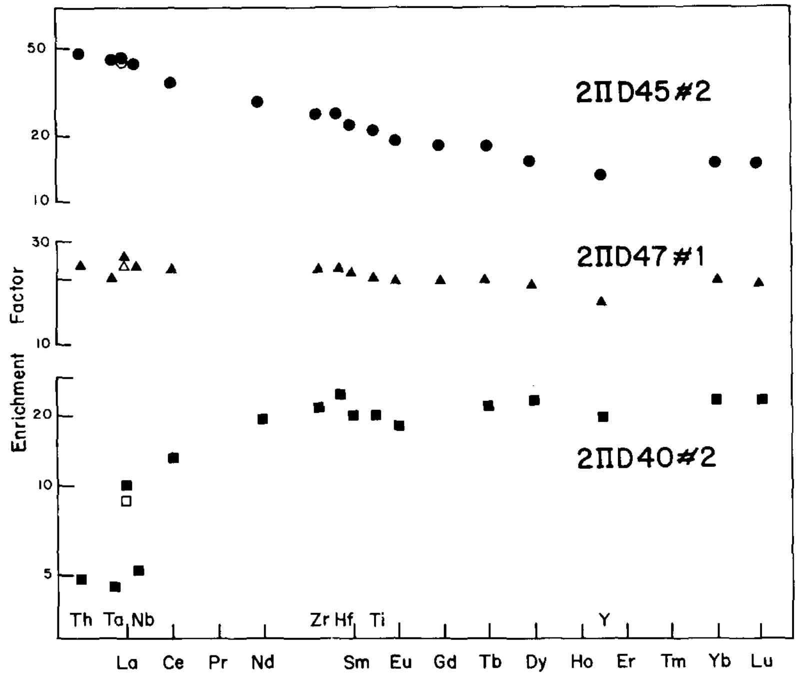

Fig. 4. "Extended" rare earth diagrams. On the x-axis, the elements are plotted versus their magmaphile character, decreasing from left to right. This classification reflects both the effects of Goldsmidt's [35] crystal chemistry prediction and of the complex formation in silicate melts [13,23,36–39]. La, Ta and Nb behave exactly the same way in MORBs that display flat to enriched patterns; we observe systematically a negative Nb, Ta anomaly for MORBs that have depleted patterns. From this last observation, $(Nb/Zr)_N$ and $(Ta/Hf)_N$ show a wider variation than $(La/Sm)_N$ in the field of depleted MORBs. The La data come from both U.R.I. (filled symbols) and P. Sue (open symbols).

type of basalts located on the 14°N segment (sample 2ΠD 45-2), the depleted character of basalts located immediately south of the Marathon Fracture Zone (sample 2ΠD 40-2) and a nearly flat pattern observed just north of the 15°20′N Fracture Zone (sample 2ΠD 47).

The above results suggest that the total along-strike length of the 14°N geochemical anomaly would not appear to exceed 450 km and could be less if no gradient exists across the 15°20′N Fracture Zone. The anomaly thus resembles the spike-like anomalies found facing the Circe (Ascension), St. Helena and Tristan da Cunha off-ridge hotspots in the South Atlantic [14], and the anomaly at the latitude of Oceanographer Fracture Zone in the North Atlantic [3,16]. But, in contrast to the other areas along the MAR, the variability of the trace element ratios along the 14°N segment, where only enriched samples where collected, is small, not exceeding some 25%; all $(Nb/Zr)_N$ ratios range from 1.5 to 1.9 with one exception (1.2 for sample 2ΠD 43-3, Table 1). Thus with regard to variability, the anomaly on the 14°N MAR segment, would seem to be more like that found in a single dredge haul in the Atlantic along segments displaying geochemical gradients about ridge-centered hotspots, such as Iceland or the Azores [1,3].

Petrological parameters or correlations based on the glass compositions of mid-oceanic ridge samples [40–43] also discriminate basalts erupted along the 14°N segment from those located north of 15°20′N Fracture Zone and south of the Marathon Fracture Zone. As an example, discriminant D [47,48] are reported in Table 1 and can be compared to $(Nb/Zr)_N$ or $(Ta/Hf)_N$.

In summary, the enriched $(Nb/Zr)_N$, $(Ta/Hf)_N$ and $(La/Sm)_N$ ratios of the 14°N MAR segment relative to adjacent segments reveal a distinct anomaly resulting from mantle heterogeneity. This interpretation has been recently confirmed with Sr and Nd isotopic ratios [44]. It remains to be shown whether the anomaly is strictly confined to the 14°N MAR segment located between

15°20′N Fracture Zone and the Marathon Fracture Zone, or is more gradational, overlapping and extending beyond the 15°20′N Fracture Zone.

5. Possible cause of the 14°N MAR anomaly

Several models are currently in vogue [45] to explain the kind of geochemical and petrological characteristics such as we have noted along the MAR in the vicinity of 14°N. These include:

(1) The plum-pudding or marble-cake model: this model was introduced to account for different signatures of mantle heterogeneity found at a local scale (e.g., a seamount) [46,47]. Small mantle domains of various shapes are randomly and passively enbedded in a depleted upper mantle.

(2) The passive heterogeneity model [16]: it differs from the previous model mainly in the size of the domains. It assumes that fairly large isolated anomalous domains are entrained in the upwelling MORB mantle.

(3) Mixing to various degrees of a buoyant, enriched plume, or chain of blobs, with the depleted asthenosphere which they penetrate. In this latter model, different dynamic or tectonic conditions have been evoked to account for the large geochemical and bathymetric anomalies along the strike of the ridge, as well as for extent of mixing and geochemical dispersion. Some of these factors include (a) spreading rates as a measure of convective upper mantle overturn rates and stirring [48], or (b) on-ridge versus off-ridge hotspot tectonic configuration, or distance of plumes to ridge axes, including the plume-source migrating-ridge sink model [11].

(4) Some "surface effects" (e.g.: cold edge effect by fracture zones); different mantle domains can be characterized by different melting points; the zero age thermal gradient is expected to change as a ridge-fracture zone intersection is approached [18]; as a consequence, liquids can be produced in different proportions from the different mantle domains present, which, in the end, can be reflected in the basalts at the surface [19,49].

None of these models appears to be entirely satisfactory for explaining the geochemical and topographic observations made near 14°N. The low variability of magmaphile element ratios such as $(Nb/Zr)_N$ over more than 110 km of the 14°N segment is hardly compatible with the high degree of freedom of the plum-pudding or marble-cake model. The effect of fracture zones on the ratio of enriched domains to depleted matrix being melted can be ruled out, since in this model, the anomaly should increase toward the fracture zones bracketing the 14°N MAR segment (Fig. 3). The alternative possibility proposed by Langmuir et al. [19], that fracture zone spacing, and geochemical anomalies possibly confined to inter fracture zone segments may reflect the scale of underlying mantle convective cells, should remain an open question. Finally, the effect of average spreading rates on the image of mantle heterogeneities, as seen in the basalts, does not apply here over so limited a distance (12°N to 17°N).

The influence from any radial dispersion over time of an intra-plate plume, such as possibly rising for example beneath the Cape Verde Islands, would create a much broader and probably more subdued geochemical anomaly along the MAR axis, judging from recent observations made in the South Atlantic [14,15]. The fixed plume source, migrating-ridge sink and connecting channel model [11] must also be excluded since, in this model, the along-strike length of the observed anomaly would require a hotspot 500 km east of the axis of the MAR, or the MAR would have overridden such a hotspot some 100 My ago [11]. In fact, the nearest proposed hotspot (Cape Verde) is at distance of some 1800 km and was overridden by the MAR between 120 and 150 My ago [50].

Two other possibilities for interpreting the 14°N geochemical anomaly concern a passive heterogeneity within the convecting mantle or a ridge-centered plume at 14°N.

The length of the 14°N anomaly along strike means that the passive heterogeneity model would require a fairly large mantle domain. Plate tectonic readjustments and triple junction relocation at 14°N could have triggered or facilitated the construction of the 14°N elevation anomaly and the off axis structures close to this latitude. To fit our geochemical data, such constructional volcanism at 14°N would have to be derived from an enriched mantle domain. This proposition raises the question about the role that plate readjustments could play at depth in the vicinity of plate boundaries, and how they would facilitate the upwelling of material derived from a hot enriched embedded mantle domain whenever present.

The alternative model, the ridge centered plume, would be consistent with the fact that some triple junctions appear to have been triggered by the rise of a mantle plume upwelling [51]. However, if this model is invoked, the lack of a pronounced elevation anomaly, such as found over the Azores or Iceland, would require that the plume has reached the upper mantle recently and that the triple junction is embryonic. This is not an impossibility: the low earthquake activity between the North and South American plates has made it difficult to locate the boundary and its intersection with the MAR axis. Clearly the embryonic plume model for 14° N is highly speculative and is considered here as an hypothesis for testing.

An ideal model would explain the relationship between the geochemical anomaly and the tectonic features and events in the area, notably the 14° N topographic high, and possibly the east-west volcano-tectonic complex as well as changes in the direction of plate motion. The passive heterogeneity and embryonic mantle plume models have quite different implications concerning the question of whether the upwelling of anomalous mantle is the effect or cause of plate readjustments.

Acknowledgements

We are grateful to the Captain and the crew of the R/V "Akademik Boris Petrov" who made this first scientific cruise of the ship a success. A special acknowledgment is due to those who installed on board the IFREMER container for analytical chemistry. P. Cambon was in charge of the preparation of the geochemical equipment, participated in the first half of the cruise and produced part of the shipboard data. We thank P. Sarda for his contribution to the measurements and for scientific discussions. We particularly thank G. Udinsev, Nadia Susheskaya and S. Cilandev for stimulating discussions and active contributions at sea. L. Dosso and C. Langmuir discussed the paper and improved the manuscript. Discussions with J. Olivet, J.C. Sibuet and B. Collette on kinematics are acknowledged. We thank B. McCully and F. Di Meglio and his staff at RINSC for neutron activation analyses and facilities. Part of this work was supported by NSF.

Academician Barsukov (Vernadsky Institute of Geochemistry), Y. Sillard (IFREMER) and C.J. Allègre (IPGP) encouraged the cooperation that led to French participation on board the R/V "Akademik Boris Petrov".

References

1 J.G. Schilling, Iceland mantle plume: geochemical evidence along Reykjanes Ridge, Nature 242, 565–571, 1973.
2 S.R. Hart, J.G. Schilling and J.L. Powell. Basalts from Iceland and along the Reykjanes Ridge: Sr isotope chemistry, Nature 246, 104–105, 1973.
3 J.G. Schilling, Azores Mantle blob: rare earth evidence, Earth Planet. Sci. Lett. 25, 103–115, 1975.
4 W.M. White and J.G. Schilling, the nature and origin of geochemical variation in Mid-Atlantic Ridge basalts from the central North Atlantic, Geochim. Cosmochim. Acta 42, 1501–1516, 1978.
5 H. Bougault and M. Treuil, Mid-Atlantic Ridge: zero-age geochemical variations between Azores and 22° N, Nature 286, 209–212, 1980.
6 P. Richard, N. Shimizu and C.J. Allègre, $^{143}Nd/^{146}Nd$, a natural tracer: an application to oceanic basalts, Earth Planet. Sci. Lett. 31, 269–278, 1976.
7 R.K. O'Nions, P.J. Hamilton and N.M. Evensen, Variations in $^{143}Nd/^{144}Nd$ and $^{87}Sr/^{86}Sr$ ratios in oceanic basalts, Earth Planet. Sci. Lett. 34, 13–22, 1977.
8 J.R. Cochran and M. Talwani, Gravity anomalies, regional elevations, and the deep structure of the North Atlantic, J. Geophys. Res. 83, 4907–4924, 1978.
9 C. Bowin, G. Thompson and J.G. Schilling, Residual geoid anomalies in the Atlantic Ocean basin: relationship to mantle plumes, J. Geophys. Res. 89, 9905–9918, 1984.
10 H. Bougault and S. Cande, Background, objectives and summary of principal results: Deep Sea Drilling Project, Sites 556–564, Init. Rep. DSDP 82, 5–16, 1985.
11 J.G. Schilling, Upper mantle heterogeneities and dynamics, Nature 314, 62–67, 1985.
12 B. Dupré and C.J. Allègre, Pb-Sr isotope variation in Indian Ocean basalts and mixing phenomena, Nature 303, 142–146, 1083.
13 H. Bougault, J.L. Joron, M. Treuil and R. Maury, Local versus regional mantle heterogeneities: evidence from hygromagmaphile elements, Init. Rep. DSDP 82, 459–482, 1985.
14 J.G. Schilling, G. Thompson, R. Kingsley and S. Humphris, Hotspot-migrating ridge interaction in the South Atlantic, Nature 313, 187–191, 1985.
15 B.B. Hanan, R.H. Kingsley and J.G. Schilling, Migrating ridge–hotspot interaction: Pb isotope evidence in the South Atlantic, Nature 332, 137–144, 1986.
16 S.B. Shirey, J.F. Bender and C.H. Langmuir, Three component isotopic heterogeneity near Oceanographer Fracture Zone, Mid-Atlantic Ridge, Nature 325, 217–223, 1987.
17 J.B. Minster and T.H. Jordan, Present day plate motions, J. Geophys. Res. 83, 5331–5354, 1978.
18 P.J. Fox and D.G. Gallo, A tectonic model for ridge-trans-

form-rid plate boundaries: implications for the structure of the oceanic lithosphere, Tectonophysics 104, 205–242, 1984.
19 C.H. Langmuir and J.F. Bender, The geochemistry of oceanic basalts in the vicinity of transform faults: observations and implications, Earth Planet. Sci. Lett. 69, 107–1127, 1984.
20 W.R. Roest and B.J. Collette, The 15° 22′N Fracture Zone and the North American/South American plate boundary, J. Geol. Soc. London 143, 833–843, 1986.
21 B.J. Collette, A.P. Slootweg, J. Verhoef and W.R. Roest, Geophysical investigations of the floor of the Atlantic Ocean between 10 and 38° N (Kroonvlag Project), Proc. K. Akad. Wet. Ser. B87, 1–76, 1984.
22 S. Le Douaran and J. Francheteau, Axial depth anomalies from 10° to 50° north along the Mid-Atlantic Ridge: correlation with other properties, Earth Planet. Sci. Lett. 54, 29–47, 1981.
23 H. Bougault, Contribution des éléments de transition à la compréhension de la genèse des basaltes océaniques. Analyse des éléments traces dans les roches par spectrométrie de fluorescence X, 221 pp., Thèse d'Etat, Université Paris VII, 1980.
24 H.D. Needham, Distribution of depths associated with accretion along the crest of the Mid-Atlantic Ridge between 41° N and 10° N, Terra Cognita 1, 36–73, 1981.
25 P. Gente, Etude morphostructurale comparative de dorsales océaniques à taux d'expansion variés, 346 pp., Thèse, Université de Brest, 1987.
26 M. Javoy and F. Pineau, The volatile record of a "popping" rock from the Mid-Atlantic Ridge at 15° N: concentrations and isotopic compositions, EOS 67, 410, 1986.
27 H. Bougault and P. Cambon, Dispersive X-ray fluorescence analysis on board oceanographic vessels, Mar. Geol. 15, 37–41, 1973.
28 H. Bougault, Major elements: analytical chemistry on board and preliminary results. Init. Rep. DSDP 37, 643–652, 1977.
29 H. Bougault, P. Cambon and H. Toulhouat, X-ray spectrometric analysis of trace elements in rocks. Correction for instrumental interferences, X-ray Spectrom. 6(2), 66–72, 1977.
30 J. Etoubleau, H. Bougault, M. Rideout, J. Brannon and B. Weaver, Analysis of trace elements in basalts by shipboard X-ray spectrometry: a discussion for Niobium, Init. Rep. DSDP 82, 35–43, 1985.
31 J.G. Schilling and W.I. Ridley, Volcanic rocks from DSDP Leg 29: petrography and rare earth abundances, Init. Rep. DSDP 29, 1103–1108, 1975.
32 H. Jaffrezic, J.L. Joron and M. Treuil, Trace element determination in rock powders: a study of the precision of a given analytical procedure—instrumental neutron activation, J. Radioanal. Chem. 39, 185–188, 1977.
33 J. Etoubleau, O. Corre, J.L. Joron, H. Bougault and M. Treuil, Costa Rica Rift: variably depleted basalts in the same hole, Init. Rep. DSDP 69, 765–773, 1983.
34 E. Tual, B.M. Jhan, H. Bougault and J.L. Joron, Geochemistry of basalts from 504B, Leg 83, Costa Rica Rift, Init. Rep. DSDP 83, 201–214, 1985.
35 D.T. Goldsmidt, The principles of distribution of the elements in minerals and rocks, J. Chem. Soc., pp. 655–672, 1937.
36 A.E. Ringwood, The principles governing trace element behaviour during magmatic crystallization, II. The role of complex formation, Geochim. Cosmochim. Acta 7, 242–254, 1955.
37 J.G. Schilling and J.W. Winchester, Rare earth contribution to the origin of Hawaiian Lavas, Contrib. Mineral. Petrol. 23, 27–37, 1969.
38 M. Treuil, Critères pétrologiques, géochimiques et structuraux de la genèse et de la différenciation des magmas basaltiques: exemple de l'Afar, 491 pp., Thèse d'Etat, Université d'Orléans, 1973.
39 M. Treuil, H. Jaffrezic, B. Villemant and G. Callas, Géochimie des éléments hygromagmatophiles, coefficients de partage minéraux/liquides et propriétés structurales de ces éléments dans les liquides magmatiques, Bull. Mineral. 102, 402–409, 1979.
40 W.G. Melson and T. O'Hearn, Basaltic glass erupted along the Mid-Atlantic Ridge between 0 and 37° N: relationships between composition and latitude, in: Deep Drilling Results in the Atlantic Ocean: Ocean Crust, M. Talwani et al., eds., Am. Geophys. Union, Maurice Ewing Ser. 2, 249–261, 1979.
41 C.H. Langmuir, J.F. Bender and R. Batiza, Petrological and tectonic segmentation of the East Pacific Rise, 5° 30′–14° 30′N, Nature, 332, 422–429, 1986.
42 N.M. Suschevskaya, L.V. Dmitriev and Sobolev, Petrological criterion for quenched abyssal glasses classification, Dokl. Acad. Sci. USRR, Earth Sci. Sect. 268(6), 1475–1477, 1983.
43 L.V. Dmitriev, A.S. Sobolev, N.M. Suschevskaya and S.A. Zapunny, Abyssal glasses, petrologic mapping of the Ocean floor and "geochemical Leg" 82, Init. Rep. DSDP 82, 509–518, 1985.
44 L. Dosso and H. Bougault, A hot spot at 14° N? Isotopic and trace element data, EOS 67, 410, 1986.
45 H. Bougault, S.C. Cande, J.G. Schilling, D.L. Turcotte and P. Olson, Mantle heterogeneity and convection, Nature 305, 278–279, 1983.
46 A. Zindler, H. Staudigel and R. Batiza, Isotope and trace element geochemistry of young Pacific Seamounts: implications for the scale of the upper mantle heterogeneity, Earth Planet. Sci. Lett. 70, 175–195, 1984.
47 N.H. Sleep, Tapping of magmas from ubiquitous Mantle heterogeneities, an alternative model to mantle plumes?, J. Geophys. Res. 89, 10,029–10,041, 1984.
48 B. Hamelin, B. Dupré and C.J. Allègre, Lead Strontium isotopic variations along the East Pacific Rise and the Mid-Atlantic Ridge: a comparative study, Earth Planet. Sci. Lett. 67, 340–350, 1984.
49 G.N. Hanson, Geochemical evolution of the sub-oceanic mantle, J. Geol. Soc. London 134, 235–260, 1977.
50 W.J. Morgan, Hotspot tracks and the early rifting of the Atlantic, Tectonophysics 94, 123–139, 1983.
51 K. Burke and J.F. Dewey, Plume generated triple junctions: key indicators in applying plate tectonics to older rocks, J. Geol. 81, 406–433, 1973.